

# Analysis of Cardiac Pulse Arrival Time Series at Rest and during Physiological Stress

Chiara Barà

Department of Engineering  
University of Palermo  
Palermo, Italy

[chiara.bara@community.unipa.it](mailto:chiara.bara@community.unipa.it)

Riccardo Pernice

Department of Engineering  
University of Palermo  
Palermo, Italy

[riccardo.pernice@unipa.it](mailto:riccardo.pernice@unipa.it)

Laura Sparacino

Department of Engineering  
University of Palermo  
Palermo, Italy

[laura.sparacino@unipa.it](mailto:laura.sparacino@unipa.it)

Yuri Antonacci

Department of Physics and  
Chemistry 'Emilio Segrè',  
University of Palermo  
Palermo, Italy

[yuri.antonacci@unipa.it](mailto:yuri.antonacci@unipa.it)

Michal Javorka

Department of Physiology and  
Biomedical Center Martin  
Jessenius Faculty of Medicine,  
Comenius University  
Martin, Slovakia

[michal.javorka@uniba.sk](mailto:michal.javorka@uniba.sk)

Luca Faes

Department of Engineering  
University of Palermo  
Palermo, Italy

[luca.faes@unipa.it](mailto:luca.faes@unipa.it)

**Abstract**— The study of cardiovascular dynamics is pivotal in the prevention and monitoring of cardiovascular diseases. Pulse Arrival Time (PAT) series contain information concerning not only the dynamics of the Autonomic Nervous System (ANS), but of all the systems involved in the regulation of cardiovascular homeostasis. This study aims to highlight how indexes extracted from PAT series in time-, frequency- and information-domain allow to discriminate among different physiological conditions. Analyses were carried out on 76 young healthy subjects, at rest and during orthostatic or mental stress. Our results show that PAT indexes vary according to the ANS condition, and may thus be useful parameters for the classification of physiological stress.

**Keywords**—Pulse Arrival Time (PAT), Electrocardiography (ECG), Blood Pressure (BP), Time series analysis, entropy

## I. INTRODUCTION

Physiological regulation in humans includes several interconnected control mechanisms that permit to maintain cardiovascular homeostasis. Mechanical, neural and hormonal factors result in variations in heart rate, blood pressure, blood flow and breathing rate that are finely connected to each other by complex dynamics [1]–[4]. To study such mechanisms, different parameters can be monitored on a beat-to-beat basis. Among them, Heart Rate Variability (HRV) is the most used parameter for the assessment of the complex dynamics underlying the cardiovascular control [5], [6]. Other measures, such as the Pulse Arrival Time (PAT), can provide information not only on the regulatory activity of the autonomic nervous system (ANS), but also on variations of blood pressure (BP) [7] and arterial stiffness [8]. The PAT is the time delay between the electrical depolarization of the heart left ventricle and the following time of arrival of the pressure wave at the body periphery [7].

Cardiovascular diseases (CVDs) represent nowadays a major cause of death and chronic disability in the world and an early diagnosis for individuals who are at a high risk of developing CVDs could permit to implement prevention strategies [9]. Some studies demonstrate how, among the different cardiovascular parameters, also the PAT and its components could be pivotal in the diagnosis of CVDs, e.g. atherosclerosis [10] and ischemic stroke [11], or of events related to them, e.g. obstructive sleep apnea [12]. In addition

to standard measurements in the time and frequency domains, the development of advanced methods for time series analysis in the information-theoretic domain provides further capability to detect and classify altered physio-pathological states [6], [13]. Moreover, the ease of implementation of algorithms capable of performing such analyses on portable devices constitutes a precious advantage for monitoring and also for early diagnosis of CVDs [14], [15]. In this sense, HRV indices have been employed not only as marker of ANS functioning, but also to estimate CVD risk [16]. Frequency domain indices such as the Low Frequency (LF, range 0.04-0.15 Hz) and High Frequency (HF, range 0.15-0.4 Hz) spectral powers have been employed not only to assess ANS activity [5], but also to extract physiological information on pulse activity [17].

In this context, the present study carries out a thorough investigation on PAT variability, computing several measures in time-, frequency- and information-theoretic domains in different physiological conditions with the aim of demonstrating their dependence on the stress condition, and thus to propose them as indexes to be used in addition to HRV measures for the detection and classification of altered physiological states.

## II. METHODS

### A. Subjects and experimental protocol

The analyses were performed on data belonging to a database employed in previous studies to investigate the effect of physical and mental stress on cardiovascular parameters [18], [19]. Signals were recorded on 76 young healthy subjects (32 males and 44 females; age  $18.4 \pm 2.7$  years), normotensive and with a normal body mass index ( $21.3 \pm 2.3$  kg/m<sup>2</sup>). The dataset consists of electrocardiographic (ECG) and blood pressure (BP) signals acquired synchronously with a sampling frequency of 1 kHz by using horizontal bipolar thoracic lead (CardioFax ECG-9620, NihonKohden, Japan) and the photoplethysmography volume-clamp method (Finometer Pro, FMS, Netherlands), respectively. The acquisition protocol consists of five phases: (a) baseline state (B) with subjects resting in the supine position on a motorized bed after a starting period of stabilization of physiological parameters (15 minutes); (b) head-up tilt state (T) obtained after inclination of the motorized bed to 45° so as to produce

orthostatic stress (8 minutes); (c) first recovery state (R1) in which subjects were put again in the resting supine position to recover physiological parameters (10 minutes); (d) mental arithmetic stress (M) in which the subjects, still laying in the supine position, were asked to perform sums of 3-digit number and indicate whether the number obtained was even or odd (6 minute); and (e) a final phase of recovery with subjects in the supine resting state (R2) (10 minutes).

### B. Time series extraction

The analyzed data consisted of the instants of occurrence of the R peaks in the ECG and of the systolic peaks in the blood pressure, extracted using the LabChart 8 (ECG analysis, blood pressure modules) toolbox from ADInstruments [18], [19]. Starting from such data, PAT intervals were obtained as the time difference between the time of each BP maximum and that of the preceding R peak. The RR time series were computed as the time intervals between two consecutive ECG R peaks and their mean was used to obtain the cut off frequency of PAT series spectrum.

In order to favor the fulfillment of stationarity criteria, for each physiological phase the analysis was performed on time windows covering 300 consecutive heartbeats (usually referred for HRV as “short-term” analysis [19]), appositely selected to avoid transient effects from a phase to the subsequent one. Specifically, the PAT time series were measured from signals acquired starting at  $\sim 8$  min,  $\sim 3$  min,  $\sim 3$  min,  $\sim 2$  min and  $\sim 5$  min after the beginning of each phase of the protocol. An example of the PAT time series measured in the five phases for a representative subject is reported in Fig. 1 (a).

### C. Preprocessing and Data analysis

Starting from PAT time series, the conventional time-domain analysis was performed computing average (MEAN)

and standard deviation (SD) values for each subject and experimental condition.

Before performing frequency- and information-domain analyses, PAT series were first preprocessed using a high-pass AR filter with cut-off frequency of 0.0156 times the sampling rate. Afterwards, the series were normalized to zero mean and unit variance. Spectral analysis was performed using the non-parametric Blackman-Tukey approach (Hamming window, bandwidth of 0.04 Hz) [20]. An example of power spectrum of PAT time series in each phase for a representative subject is reported in Fig. 1 (b). After obtaining the spectrum of the PAT series, frequency-domain indexes were extracted. Specifically, the LF spectral power ( $P_{LF}$ , range 0.04-0.15 Hz), the HF spectral power ( $P_{HF}$ , range 0.15-0.4 Hz) and the ratio  $P_{LF}/P_{HF}$  were computed.

Information-theoretic analysis was performed to assess the static and dynamic information content of the analyzed series. Specifically, the entropy of a process  $X$ , representing the quantity of information held in the current state of  $X$ , is defined under the hypothesis of stationarity as [21]:

$$H_X = -E[\ln p(x_n)] \quad (1)$$

being  $x_n$  the value of the most recent sample of  $X$ , and  $p(x_n)$  its probability. An example of probability distribution  $p(x_n)$ , estimated using histogram quantization of  $PAT(n)$ , is reported in Fig. 1 (c). The information storage (S) is the quantity of information held in the current state of the system attributable to its past states, measuring regularity and predictability of the time series; it is defined as follows [21]:

$$S_X = I(X_n; X_n^-) = E \left[ \ln \frac{p(x_n, x_n^-)}{p(x_n)p(x_n^-)} \right] \quad (2)$$

being  $I(\cdot; \cdot)$  the mutual information,  $X_n^- = [X_{n-1} X_{n-2} \dots]$  collects the random variables sampling the past of the

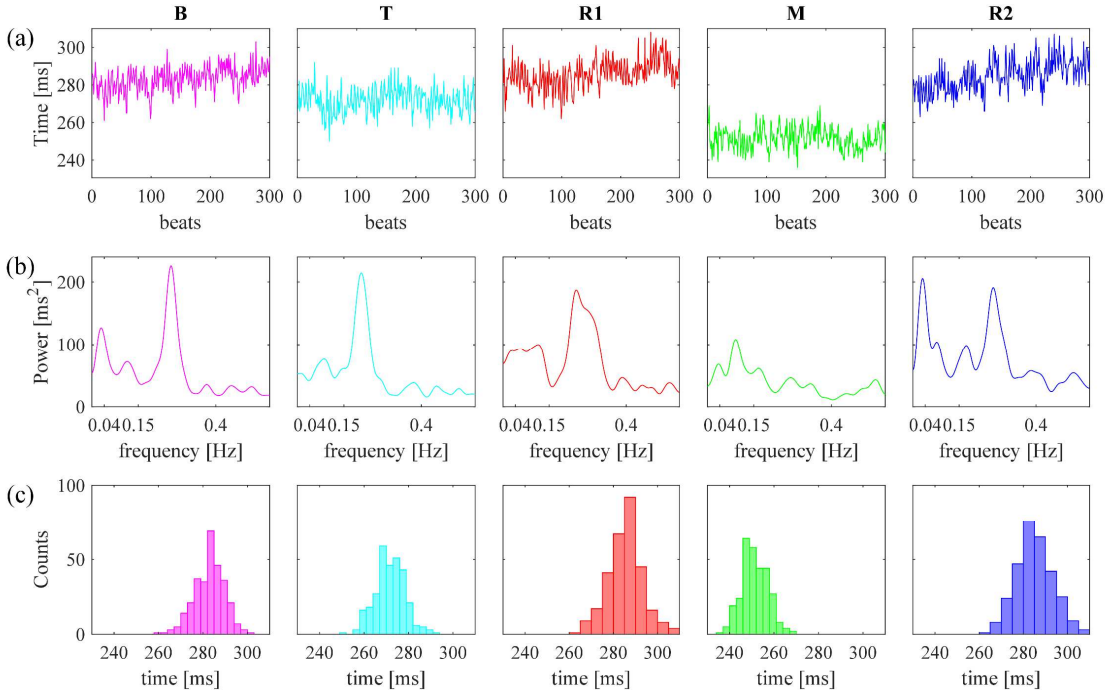


Fig. 1. Example of PAT time series (a), power spectrum (b) and probability distributions (c) for a representative subject during baseline (B), orthostatic stress (T), resting period after tilt (R1), arithmetical stress (M) and final resting period (R2). In this example, the following time-domain, frequency-domain and information-theoretic measures were computed for B, T, R1, M and R2: MEAN: 283.07, 271.82, 285.67, 251.43, 284.93 ms, SD: 6.67, 6.69, 7.74, 5.89, 8.45 ms,  $P_{LF}$ : 7.26, 6.63, 9.75, 8.40, 9.19  $\text{ms}^2$ ,  $P_{HF}$ : 17.90, 21.07, 22.74, 10.77, 22.16  $\text{ms}^2$ ,  $P_{LF}/P_{HF}$ : 0.41, 0.31, 0.43, 0.78, 0.41, H: 3.18, 3.24, 3.28, 3.11, 3.32 nats with linear estimator and 3.19, 3.21, 3.21, 3.09, 3.33 nats with knn estimator, S: 0.07, 0.08, 0.07, 0.04, 0.04 nats with linear estimator.

analyzed process, and  $x_n^- = [x_{n-1} x_{n-2} \dots]$  represents a realization of  $X_n^-$ .

These two measures were estimated using both parametric and model-free approaches. As regarding the linear parametric method, starting from the assumption that the PAT time series follows a Gaussian distribution, measures in (1) and (2) are computed as [22]:

$$\hat{H}_X = \frac{1}{2} \ln(2\pi e \hat{\sigma}_X^2) \quad (3)$$

$$\hat{S}_X = \frac{1}{2} \ln \frac{\hat{\sigma}_X^2}{\hat{\sigma}_U^2} \quad (4)$$

where  $\hat{\sigma}_X^2$  is the variance of the PAT series and  $\hat{\sigma}_U^2$  is the variance of the residuals obtained by solving a linear regression problem where  $X_n$  is predicted from  $X_n^-$ . The model order was set to 2, so that the past of the process is considered of finite length and equal to the model order, i.e.  $X_n^- \approx X_n^2 = [X_{n-1} X_{n-2}]$ . The non-parametric *k-nearest neighbor* (*knn*) estimates of information indexes were instead obtained by using the following formulation [22]:

$$\hat{H}_x = \psi(N) - \psi(k) + \langle \ln \varepsilon_n \rangle \quad (5)$$

$$\hat{S}_x = \psi(N) + \psi(k) - \langle \psi(Nx_n) \rangle - \langle \psi(Nx_n^m) \rangle \quad (6)$$

where  $\psi(\cdot)$  is the digamma function,  $N$  is the number of available observations of the present and past variables,  $k$  is the number of neighbors selected for the analysis,  $m$  is the embedding dimension, i.e. the number of time-lagged variables that approximate the past history of the process,  $\varepsilon_n$  is twice the distance from  $x_n$  to its  $k$ -th nearest neighbor in the one-dimensional space computed according to the maximum norm, and  $N_{x_n}$  and  $N_{x_n^m}$  are the number of points whose distance from  $X_n$  and  $X_n^m$  is smaller than  $\varepsilon_n/2$ , respectively. For the analyses we set the parameters to  $k=10$  and  $m=2$ , respectively, which have been proven suitable in previous studies for the analysis of short time series [19].

This selection of the parameters is also adequate for the implementation of the algorithms within the firmware of wearable devices: indeed, a fixed low AR model order as well as a small embedding vector allow to limit the computational costs.

#### D. Statistical Analysis

The statistical analyses were carried out on the distributions of all the time-domain, frequency-domain and information-theoretic domain measures using non-parametric tests. Specifically, the Kruskal-Wallis analysis of variance was employed to test for differences of the distributions among all the conditions, followed by a pairwise post-hoc Wilcoxon signed rank test. The Bonferroni-Holm correction was employed to correct for multiple comparisons ( $n=10$ ). The Wilcoxon signed rank test was also applied to determine the presence of statistically significant differences between the distributions of the two different estimates of information-domain measures (i.e. linear vs knn). For all statistical tests, the significance level was set at 0.05.

### III. RESULTS

Fig. 2 shows the results of time-domain analysis carried out on PAT time series in the five physiological conditions. With regard to MEAN (Fig. 3(a)), statistically significant differences can be observed between each pair of conditions except between B and the resting periods following the execution of tasks (R1 and R2). Specifically, the mean PAT

decreases during mental stress if compared to physical stress and even more if compared to the baseline. On the other hand, variability of PAT (Fig. 3(b)) during baseline is lower than that recorded during R1 and R2 and there is a significant increase during tilt if compared to baseline and mental stress.

Fig.3 reports the results of frequency-domain analyses, i.e. the distributions of power values in LF and HF bands and also their ratio for all the phases of the protocol. Both the LF and HF spectral powers increase significantly during T and decrease during M. No statistically significant differences are detected for  $P_{LF}/P_{HF}$  ratio, given that the trends of LF and HF powers are similar in all the considered conditions.

The distributions of information-domain indexes obtained with both linear and knn estimators are shown in Fig. 4. Significant differences can be observed both for H and S during the T and M phases if compared to rest conditions, with higher values during T and lower values during M. The use of the knn estimator leads to significantly lower values of entropy, and to significantly higher values of information storage, when compared to the linear estimator.

### IV. DISCUSSION

The present study investigates the information provided by indexes extracted from PAT time series about the complex physiological control system that leads to the achievement of cardiovascular homeostasis. By measuring the beat-to-beat variability of the time interval between the contraction of the heart and the arrival of the pulse wave in the peripheral artery, it is possible to infer information not only about the balance between the activity of the sympathetic (SNS) and parasympathetic (PNS) branches of the ANS, but also on changes in blood pressure following the baroreflex, on the influence of respiration on arterial stiffness, and therefore on all whole cardiovascular hemodynamics [4], [23].

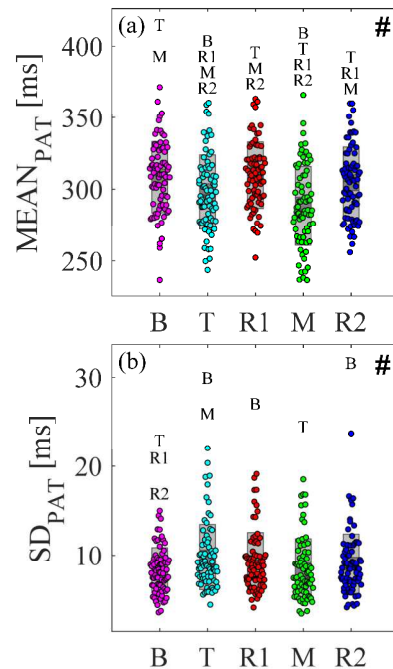


Fig. 2. Boxplots and individual values of MEAN (a) and SD (b) of PAT time series computed for all subjects during the five conditions (baseline (B), head-up tilt (T), mental arithmetic test (M) and supine rest phases (R1, R2)). Statistical analysis: #,  $p < 0.05$ , Kruskal-Wallis test; phase name,  $p < 0.05$  pairwise, Wilcoxon signed rank test with Bonferroni-Holm correction.

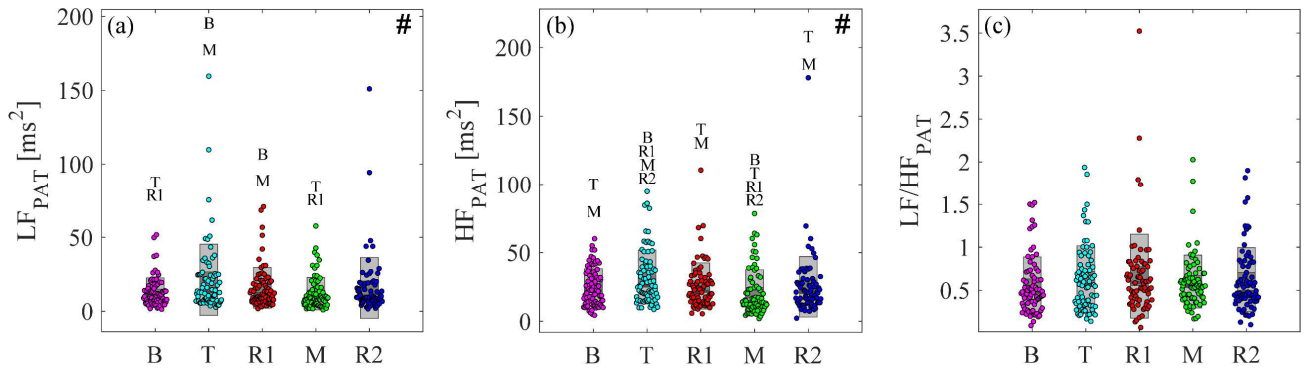


Fig. 3. Boxplots and individual values of LF power (a), HF power (b) and LF/HF power ratio (c) of PAT time series computed for all subjects during the five conditions (baseline (B), head-up tilt (T), mental arithmetic test (M) and supine rest phases (R1, R2)). Statistical analysis: #,  $p < 0.05$ , Kruskal-Wallis test; phase name,  $p < 0.05$  pairwise, Wilcoxon signed rank test with Bonferroni-Holm correction.

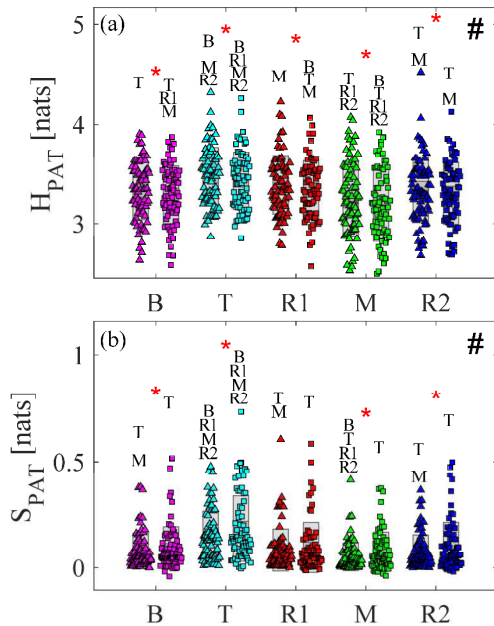


Fig. 4. Boxplots and individual values of entropy  $H$  (a) and information storage  $S$  (b) of PAT time series computed for all subjects during the five conditions (baseline (B), head-up tilt (T), mental arithmetic test (M) and supine rest phases (R1, R2)) with both linear (triangular markers on the left) and knn (square markers on the right) estimators. Statistical analysis: #,  $p < 0.05$ , Kruskal-Wallis test for both estimators; phase name,  $p < 0.05$  pairwise, Wilcoxon signed rank test with Bonferroni-Holm correction; \*,  $p < 0.05$  linear vs. knn, Wilcoxon signed rank test.

Moreover, analyzing PAT allows to distinguish the Pre-Ejection Period (PEP), i.e. the time interval between the depolarization of ventricle and the opening of the aortic valve, and the Pulse Transit Time (PTT), that is the time interval that the pressure wave takes to travel from the aortic valve to the peripheral arteries [7].

As reported in several previous studies [19], [24], the cardiovascular control system reacts to physiological stress conditions by increasing the heart rate (HR), the blood pressure and the cardiac output, but also with responses which depend on the type of stressor and thus linked to different aspects of cardiovascular regulation. This can be related to the differences shown in our results between the phases of head-up tilt and mental arithmetics. In fact, we observe how the parameters obtained during orthostatic and arithmetic stress phases present often different trends (see Figs. 2 to 4).

As indicated by the increased predictability of PAT during head-up tilt (see Fig. 4(b)), in this phase well-defined oscillatory mechanisms come into play, providing information

on the sympatho-vagal balance as demonstrated by numerous studies in the literature [6], [19]. Previous studies have also reported that the increase of the tilt angle during head-up tilt procedure causes an increase of the pre-ejection period and a decrease of the pulse transit time [25]. In this phase, venous pooling of blood to the lower limbs leads to a decrease of cardiac preload and consequently to a decrease of the contraction strength via the Frank-Starling law, with consequent increase of the PEP [26]. On the other side, the mean arterial blood pressure tends to remain constant and this can be explained by an increase of arterial stiffness [27] which leads to a decrease of the PTT; this mechanism is regulated by the arterial baroreceptors [28]. The reduction of the mean PAT (see Fig. 2(a)) mostly reflects the trend of PTT, moreover it is important to underline how mechanisms of regulation of PEP and PTT act differently for each subject and within each heartbeat, thus leading to a high variability of PAT during orthostatic stress [29] (see Fig. 2(b)). The larger variability of the PAT during this phase can be related to larger amounts of information contained in the time series, reflected in our data by the higher entropy values than those recorded in the resting phase (see Fig. 4(a)).

Previous studies focusing on HRV analyses ([19] on the same data or [30]) reported how the oscillations linked to the variability of the heart rate decrease in the HF band and increase in the LF band during the orthostatic challenge, evidencing a shift in the sympatho-vagal balance. Instead, our analysis on PAT variability evidences that power increases in both LF and HF bands (see Fig. 3(a, b)), showing thus that the most important differences with HRV are observed in HF band. Such a finding suggests that the vascular dynamics in this band are expected to be mainly driven by other mechanisms rather than by the regulation of the autonomic system. This is in agreement to previous findings in literature that describe the dynamics in the HF band is mainly related to respiratory modulation of vasoconstriction [17]. Instead, the increase of LF band power can be explained both with autonomic regulation mechanisms (basically, the sympathetic activation during tilt) but also through Mayer waves [6], [17], [31] due to baroreflex activity [2]. Our results (Fig. 3(c)) show that, unlike in HRV analysis [5], the LF / HF ratio is not indicative of the sympatho-vagal balance when studying PAT.

On the other hand, the transition from a resting state to a mental stress condition induces a decrease in the regularity of PAT, as shown in Fig. 4(b). This may be related to the presence of different control mechanisms during mental stress, not as well defined as in the case of an orthostatic challenge, possibly related to a non-stable and time-variant

cardiovascular system [32]. Previous studies suggest that, despite the increase of heart rate and of mean arterial pressure, there is not a significant change in muscle sympathetic nerve activity (MSNA) during mental stress, and thus the vascular control in the peripheral arteries is not influenced by the sympathetic outflow [33], [34]. Specifically, mental stress decreases the forearm vascular resistance leading to an increase of blood flow due to sympathetic withdrawal, active neurogenic vasodilatation and  $\beta$ -adrenergic vasodilatation [35]. Such complex regulatory mechanisms occurring during a mental stress condition produce a decrease of mean PAT (see Fig. 2(a)) linked to a decrease in PEP, due to weakening of parasympathetic activity and a positive inotropic effect [26], and to a decrease in PTT, as found in similar studies [26], [29], [36]. These two similar trends lead to a lower PAT variability during the arithmetic stress phase, as documented by our results in Fig. 2(b). Following forearm vascular dilation, we would expect an increase in PTT during the phase of mental stress compared to a condition of rest, but this is not what is shown by results. As previously discussed, cardiovascular system during a condition of mental stress is time-variant: at the beginning of the task, parasympathetic withdrawal starts to occur and sympathetic nerves are still not activated; going on with the mental stress, there is an activation of the latter, probably associated to changes of cortical potential, given by neural and cardiovascular response [32]. Therefore, one could expect that the results obtained in terms of mean PAT depend on the selection of the windows of the time series. The frequency domain analysis provides further information if compared to time-domain indices, highlighting a lower sympathetic activity during mental stress if compared to tilt (see Fig. 3(a)).

Finally, interesting remarks can be made looking at differences between linear and knn estimators in the evaluation of information-domain indexes (see Fig. 4). The higher values of information storage obtained using the knn estimator compared with the linear estimator suggest the presence of nonlinear dynamics underlying this aspect of the cardiovascular regulation [22]. A previous study combining the computation of nonparametric estimators of information measures with the method of surrogate data reported that HRV is also affected by nonlinear dynamics [37]. Although similar studies have not been carried out on PAT time series, we may speculate that this may also be true with regard to the dynamics of cardiovascular control analyzed with PAT, given that our results almost always show statistically significant differences between the values of information storage computed using linear and nonlinear estimators. While these results indicate that it would be preferable to use the non-parametric estimator to capture the complexity of PAT dynamics, the observation that the main changes with stress (T vs B and M vs R1) are detected by both estimators suggest the feasibility of a simpler linear analysis. In fact, the linear estimator may represent the best algorithm to be implemented within the firmware of portable devices, being at the same time quite reliable and requiring less computational power.

A limitation of studying PAT consists in the fact that it cannot be considered as a surrogate of PTT or of the Pulse Wave Velocity (PWV) [38], that have been used in the literature for a quite reliable assessment of blood pressure and arterial stiffness [39]. It is also important to highlight that PAT time series are usually extracted from synchronous acquisition of photoplethysmographic (PPG) and ECG signals. Instead, in this work we use timing peaks of BP signal as surrogate of

timing peaks of PPG signal. This should not affect significantly the validity of the analyses, since BP and PPG signals have similarities in terms of pulsation timing [40]. Moreover, although the absolute value of the PAT depends on the signal from which the arrival times are measured (PPG or BP), on the acquisition site (finger, toe, ear...) and on the point of signal that was considered for its determination (minimum, maximum, inflection points...), its relative changes across different phases are indicative of cardiovascular control mechanisms activity.

## V. CONCLUSIONS

This paper reports a systematic analysis of PAT series acquired during different physiological conditions, employing time-, frequency- and information-theoretic domain measures. Our results evidence that cardiovascular dynamics represented by PAT behave differently in the various conditions. Thus, the proposed indices allow to discriminate the transition from a resting to a stress state, also showing differences between physical and mental stressors. The indirect comparison with HRV indices, representing the gold standard for assessing ANS activity, showed some similarities but also different behaviors. Although the PAT does not allow to delineate precisely the heart rate dynamics, its evaluation favors a more complete understanding of the complex regulatory mechanisms that also include the dynamics of blood pressure, respiration and vascular response. This may also have clinical relevance, in terms of prevention and monitoring of CVDs. Future activities may consider to combine HRV and PAT indices, taking also into account other signals (e.g. blood pressure, respiration), together with employing novel information dynamics tools, e.g. multiscale Information Decomposition [41], to have a more comprehensive understanding of cardiovascular and cardiorespiratory dynamics.

## ACKNOWLEDGMENT

This research activity was supported by Italian Ministry of Education, University and Research “*Sensoristica intelligente, infrastrutture e modelli gestionali per la sicurezza di soggetti fragili*” (4FRAILTY) project (PON R&I ARS01\_00345). RP was supported by the Italian MIUR PON R&I 2014-2020 AIM project no. AIM1851228-2. LF and YA were supported by the Italian MIUR PRIN 2017 project 2017WZFTZP “Stochastic forecasting in complex systems”.

## REFERENCES

- [1] M. C. K. Khoo and P. Chalacheva, “Respiratory modulation of peripheral vasoconstriction: a modeling perspective,” *J. Appl. Physiol.*, vol. 127, no. 5, pp. 1177–1186, 2019.
- [2] M. A. Cohen and J. A. Taylor, “Short-term cardiovascular oscillations in man: measuring and modelling the physiologies,” *J. Physiol.*, vol. 542, no. 3, pp. 669–683, 2002.
- [3] S. C. Malpas, “Neural influences on cardiovascular variability: possibilities and pitfalls,” *Am. J. Physiol. Circ. Physiol.*, vol. 282, no. 1, pp. H6–H20, 2002.
- [4] S. Schulz *et al.*, “Cardiovascular and cardiorespiratory coupling analyses: a review,” *Philos. Trans. R. Soc. A Math. Phys. Eng. Sci.*, vol. 371, no. 1997, p. 20120191, 2013.
- [5] F. Shaffer and J. P. Ginsberg, “An overview of heart rate variability metrics and norms,” *Front. public Heal.*, p. 258, 2017.
- [6] M. Javorka *et al.*, “Towards understanding the complexity of cardiovascular oscillations: insights from information theory,” *Comput. Biol. Med.*, vol. 98, pp. 48–57, 2018.
- [7] E. Finnegan *et al.*, “Pulse arrival time as a surrogate of blood pressure,” *Sci. Rep.*, vol. 11, no. 1, pp. 1–21, 2021.
- [8] B. Paliakaitė, S. Daukantas, and V. Marozas, “Assessment of pulse

- arrival time for arterial stiffness monitoring on body composition scales,” *Comput. Biol. Med.*, vol. 85, pp. 135–142, 2017.
- [9] L. Lin, H. Wu, L. Yan, H. Wang, H. Yang, and H. Li, “Global, Regional, and National Cancer Death and Disability-Adjusted Life-Years (DALYs) for Cardiovascular Disease in 2017, and Trends, Risk Analysis, 1990 to 2017, from the Global Burden of Disease Study and Implications for Prevention,” *Risk Anal.*, 1990.
- [10] H.-L. Kim and S.-H. Kim, “Pulse wave velocity in atherosclerosis,” *Front. Cardiovasc. Med.*, vol. 6, p. 41, 2019.
- [11] A. K. Verma, P. N. Aarotale, P. Dehkordi, J.-S. Lou, and K. Tavakolian, “Relationship between ischemic stroke and pulse rate variability as a surrogate of heart rate variability,” *Brain Sci.*, vol. 9, no. 7, p. 162, 2019.
- [12] Y. Kwon *et al.*, “Pulse arrival time, a novel sleep cardiovascular marker: the multi-ethnic study of atherosclerosis,” *Thorax*, 2021.
- [13] M. Valente *et al.*, “Univariate and multivariate conditional entropy measures for the characterization of short-term cardiovascular complexity under physiological stress,” *Physiol. Meas.*, vol. 39, no. 1, p. 014002, 2018.
- [14] J. Hong, Y. Zheng, S. Wu, G. Geng, Q. Liu, and C. C. Y. Poon, “Characterization of the vascular system using overnight wearable-based pulse arrival time and ambulatory blood pressure: A pilot study,” *Comput. Biol. Med.*, vol. 137, p. 104861, 2021.
- [15] J. Lin *et al.*, “Wearable sensors and devices for real-time cardiovascular disease monitoring,” *Cell Reports Phys. Sci.*, vol. 2, no. 8, p. 100541, 2021.
- [16] Y. Kubota, L. Y. Chen, E. A. Whitsel, and A. R. Folsom, “Heart rate variability and lifetime risk of cardiovascular disease: the Atherosclerosis Risk in Communities Study,” *Ann. Epidemiol.*, vol. 27, no. 10, pp. 619–625, 2017.
- [17] J. Lázaro, R. Bailón, P. Laguna, V. Marozas, A. Rapalis, and E. Gil, “Difference in pulse arrival time at forehead and at finger as a surrogate of pulse transit time,” in *2016 Computing in Cardiology Conference (CinC)*, 2016, pp. 269–272.
- [18] M. Javorka *et al.*, “Basic cardiovascular variability signals: mutual directed interactions explored in the information domain,” *Physiol. Meas.*, vol. 38, no. 5, p. 877, 2017.
- [19] R. Pernice *et al.*, “Comparison of short-term heart rate variability indexes evaluated through electrocardiographic and continuous blood pressure monitoring,” *Med. Biol. Eng. Comput.*, vol. 57, no. 6, pp. 1247–1263, 2019.
- [20] R. B. Blackman and J. W. Tukey, “The measurement of power spectra from the point of view of communications engineering—Part I,” *Bell Syst. Tech. J.*, vol. 37, no. 1, pp. 185–282, 1958.
- [21] H. Azami, L. Faes, J. Escudero, A. Humeau-Heurtier, and L. E. V Silva, “Entropy Analysis of Univariate Biomedical Signals: Review and Comparison of Methods,” 2020.
- [22] W. Xiong, L. Faes, and P. C. Ivanov, “Entropy measures, entropy estimators, and their performance in quantifying complex dynamics: Effects of artifacts, nonstationarity, and long-range correlations,” *Phys. Rev. E*, vol. 95, no. 6, p. 062114, 2017.
- [23] A. S. Patel and K. G. Burnand, “Cardiovascular haemodynamics and shock,” *Surg.*, vol. 27, no. 11, pp. 459–464, 2009.
- [24] W. L. Wasmund, E. C. Westerholm, D. E. Watenpugh, S. L. Wasmund, and M. L. Smith, “Interactive effects of mental and physical stress on cardiovascular control,” *J. Appl. Physiol.*, vol. 92, no. 5, pp. 1828–1834, 2002.
- [25] G. S. H. Chan, P. M. Middleton, B. G. Celler, L. Wang, and N. H. Lovell, “Change in pulse transit time and pre-ejection period during head-up tilt-induced progressive central hypovolaemia,” *J. Clin. Monit. Comput.*, vol. 21, no. 5, pp. 283–293, 2007.
- [26] J. Krohová, B. Czipelová, Z. Turianiková, Z. Lazarová, I. Tonhajzerová, and M. Javorka, “Preejection period as a sympathetic activity index: a role of confounding factors,” 2017.
- [27] V. L. Cooper and R. Hainsworth, “Carotid baroreceptor reflexes in humans during orthostatic stress,” *Exp. Physiol.*, vol. 86, no. 5, pp. 677–681, 2001.
- [28] V. L. Cooper and R. Hainsworth, “Effects of head-up tilting on baroreceptor control in subjects with different tolerances to orthostatic stress,” *Clin. Sci.*, vol. 103, no. 3, pp. 221–226, 2002.
- [29] G. Mijatovic *et al.*, “Measuring the Rate of Information Exchange in Point-Process Data with Application to Cardiovascular Variability,” *Front. New. Physiol.*, vol. 1, 2022.
- [30] K. Efremov *et al.*, “Heart rate variability analysis during head-up tilt test predicts nitroglycerine-induced syncope,” *Open Hear.*, vol. 1, no. 1, p. e000063, 2014.
- [31] A. Porta, T. Gnecci-Ruscione, E. Tobaldini, S. Guzzetti, R. Furlan, and N. Montano, “Progressive decrease of heart period variability entropy-based complexity during graded head-up tilt,” *J. Appl. Physiol.*, vol. 103, no. 4, pp. 1143–1149, 2007.
- [32] X. Wang, B. Liu, L. Xie, X. Yu, M. Li, and J. Zhang, “Cerebral and neural regulation of cardiovascular activity during mental stress,” *Biomed. Eng. Online*, vol. 15, no. 2, pp. 335–347, 2016.
- [33] J. R. Carter and C. A. Ray, “Sympathetic neural responses to mental stress: responders, nonresponders and sex differences,” *Am. J. Physiol. Circ. Physiol.*, vol. 296, no. 3, pp. H847–H853, 2009.
- [34] N. T. Kuipers, C. L. Sauder, J. R. Carter, and C. A. Ray, “Neurovascular responses to mental stress in the supine and upright postures,” *J. Appl. Physiol.*, vol. 104, no. 4, pp. 1129–1136, 2008.
- [35] J. R. Halliwill, L. A. Lawler, T. J. Eickhoff, N. M. Dietz, L. A. Nauss, and M. J. Joyner, “Forearm sympathetic withdrawal and vasodilatation during mental stress in humans,” *J. Physiol.*, vol. 504, no. 1, pp. 211–220, 1997.
- [36] S. L.-O. Martin *et al.*, “Weighing scale-based pulse transit time is a superior marker of blood pressure than conventional pulse arrival time,” *Sci. Rep.*, vol. 6, no. 1, pp. 1–8, 2016.
- [37] L. Faes *et al.*, “Comparison of methods for the assessment of nonlinearity in short-term heart rate variability under different physiopathological states,” *Chaos An Interdiscip. J. Nonlinear Sci.*, vol. 29, no. 12, p. 123114, 2019.
- [38] F. Beutel, C. Van Hoof, X. Rottenberg, K. Reesink, and E. Hermeling, “Pulse Arrival Time Segmentation into Cardiac and Vascular Intervals—Implications for Pulse Wave Velocity and Blood Pressure Estimation,” *IEEE Trans. Biomed. Eng.*, 2021.
- [39] R. Mukkamala *et al.*, “Toward ubiquitous blood pressure monitoring via pulse transit time: theory and practice,” *IEEE Trans. Biomed. Eng.*, vol. 62, no. 8, pp. 1879–1901, 2015.
- [40] J. Allen, “Photoplethysmography and its application in clinical physiological measurement,” *Physiol. Meas.*, vol. 28, no. 3, p. R1, 2007.
- [41] J. Krohova *et al.*, “Multiscale information decomposition dissects control mechanisms of heart rate variability at rest and during physiological stress,” *Entropy*, vol. 21, no. 5, p. 526, 2019.